

From single-particle to collective effective temperatures in an active fluid of self-propelled particles

DEMIAN LEVIS¹ and LUDOVIC BERTHIER²

¹ *Departament de Física Fonamental, Universitat de Barcelona, Av. Diagonal 645, E08028 Barcelona, Spain*

² *Laboratoire Charles Coulomb, UMR 5221, CNRS and Université Montpellier, Montpellier, France*

PACS 05.10.Ln – Monte-Carlo methods

PACS 47.57.-s – Complex fluids and colloidal systems

Abstract – We present a comprehensive analysis of effective temperatures based on fluctuation-dissipation relations in a model of an active fluid composed of self-propelled hard disks. We first investigate the relevance of effective temperatures in the dilute and moderately dense fluids. We find that a unique effective temperature does not in general characterize the non-equilibrium dynamics of the active fluid over this broad range of densities, because fluctuation-dissipation relations yield a lengthscale-dependent effective temperature. By contrast, we find that the approach to a non-equilibrium glass transition at very large densities is accompanied by the emergence of a unique effective temperature shared by fluctuations at all lengthscales. This suggests that an effective thermal dynamics generically emerges at long times in very dense suspensions of active particles due to the collective freezing occurring at non-equilibrium glass transitions.

Introduction. – Statistical mechanics provides a unified theoretical description of systems at thermal equilibrium in terms of the probability distribution over phase space, from which thermodynamic quantities such as temperature can be defined [1]. A similar framework is lacking for out-of-equilibrium systems for which the definition of a temperature remains an open issue [2]. Active matter formed by assemblies of living cells [3], bacteria [4], self-propelled colloids [5–8] or grains [9, 10], is a coherent class of non-equilibrium systems receiving increasing attention, because they raise fundamental issues and for potential applications in soft matter and biophysics [11, 12]. A number of recent studies have addressed the question of whether “effective” thermodynamic concepts can be fruitfully applied to describe the phase behaviour and microscopic dynamics of active matter. This question is natural because if some mapping to an equilibrium situation exists, then the whole arsenal of equilibrium statistical mechanics becomes available for further theoretical treatment. In particular the definition of a non-equilibrium temperature [13–18], of an active pressure [8, 19, 20], of activity-induced interactions [8, 21] and non-equilibrium free energies [22, 23] have been investigated for self-propelled particles.

An effective temperature T_{eff} defined as the parameter replacing the thermal bath temperature in fluctuation-

dissipation relations was extensively studied in slowly relaxing materials, such as spin and structural glasses [24–27]. In these systems, the effective temperature becomes a meaningful thermodynamic concept [28]. It can be used to quantify heat flows and can be defined through a microcanonical construction over a restricted region of the phase space. Physically, this approach is possible because there is a strong decoupling of timescales [2] between thermal motion at short times, which essentially follows an equilibrium statistics, and an “effective” thermal dynamics at long times, which is an emerging collective property characterizing slow dynamical events leading to structural relaxation in driven and aging glasses.

In active matter, the possibility to define a *single-particle* effective temperature in the dilute regime where particles do not interact has been discussed [14, 16, 17, 29, 30]. The simple fluid state has been analysed mostly by numerical simulations determining fluctuation-dissipation relations for different observables in various models of self-propelled particles [13, 15, 18]. Finally, in the limit of very large densities where self-propelled particles may undergo a non-equilibrium glass transition, the driven glassy dynamics should resemble the one of slowly driven glasses and a *collective* effective temperature was predicted to emerge from the analysis of a mean-field active glass model [31], but this prediction has not been tested in a re-

alistic model in finite dimension. In this work, we focus on a model of an active fluid composed of self-propelled hard disks and analyse fluctuation-dissipation relations over a very broad range of densities encompassing the dilute, fluid and glassy regimes, in order to provide a comprehensive picture of the relevance of effective temperatures in active matter. In particular, we find strong violations to the fluctuation-dissipation relations in all regimes, but conclude that effective temperatures appear most relevant in the slowly relaxing glassy regime.

Numerical model. – We consider a two-dimensional system of N interacting self-propelled hard disks of diameter σ , enclosed in a $L \times L$ square box with periodic boundary conditions. Self-propulsion is modelled by a non-Markovian stochastic drive, implemented by a kinetic Monte-Carlo (MC) rule that we describe below. The phase behaviour of the model and its microscopic dynamics were investigated before [8,32,33]. Here we extend these studies to analyse fluctuation-dissipation relations and effective temperatures over a large range of densities.

A particle configuration is described by $\{\mathbf{r}_i(t), i = 1 \dots N\}$, the set of particle positions at time t . The dynamics proceeds as follows. At time t , a particle i is chosen at random and a small displacement $\delta_i(t)$ of amplitude $|\delta_i(t)| < \delta_0$ is proposed. Just as for equilibrium hard disks [34], the particle position is updated according to $\mathbf{r}_i(t + \Delta t) = \mathbf{r}_i(t) + \delta_i(t)P_{\text{hard}}$, where $P_{\text{hard}} = 1$ if the move does not generate any overlap with a neighbouring disk, and $P_{\text{hard}} = 0$ otherwise.

Self-propulsion is introduced via a finite persistence time of the successive moves $\delta_i(t)$. This non-Markovian dynamics breaks detailed balance. In practice, we choose $\delta_i(t + \Delta t) = \delta_i(t) + \boldsymbol{\eta}_i(t)$, where $\boldsymbol{\eta}_i(t)$ is a uniformly distributed random shift of amplitude $|\boldsymbol{\eta}_i(t)| < \delta_1$, chosen independently at each step. As a consequence, successive displacements δ_i decorrelate after a persistence time $\tau = (\delta_0/\delta_1)^2$, and this dynamics generates persistent random walks for isolated particles. (See Ref. [32] for more details about the model.) This model is appealing because it has only two control parameters. The persistence time τ controls the self-propulsion of the particles, whereas the packing fraction $\varphi = \frac{\pi N \sigma^2}{4L^2}$ quantifies excluded volume effects. In addition, the equilibrium hard disk model, where the physics is uniquely controlled by φ , is restored in the limit $\tau \rightarrow 0$. The model does not include more complex features such as alignment rules or hydrodynamic interactions and serves as a minimal model to study the direct competition between glassiness and self-propulsion. A continuous-time version of the model for arbitrary particle interactions has recently appeared [35].

We perform simulations using $N = 10^3$ particles, varying φ and τ . We vary φ from the dilute limit $\varphi \rightarrow 0$ up to $\varphi = 0.825$, well beyond the equilibrium glass transition of hard disks $\varphi_c^{\text{eq}} \approx 0.80$ [36], and τ in the range $\tau \in [0, 10^4]$. We fix for convenience $\delta_0 = \sigma/10$. From now on, we set the Boltzmann constant $k_B = 1$, we use σ as the unit of

length and one MC step represents N attempted moves. To suppress crystallisation in the glassy regime, we use a 35:65 binary mixture of hard disks with diameter ratio $\sigma_1/\sigma_2 = 1.4$ (σ_1 then being the unit length) for systems above $\varphi = 0.69$. For lower φ , all systems are monodisperse. Size polydispersity is introduced for convenience, but it does not influence the results presented below.

Fluctuation-dissipation relations. – Using linear response theory at equilibrium, one can prove that the response of a system to an infinitesimal external perturbation is related to the spontaneous fluctuations of its conjugate observable via the fluctuation-dissipation theorem (FDT) [1]. Consider a system perturbed at time $t = 0$ by an external field of constant amplitude f_0 coupled to an observable B . We define the cross-correlation function between observables $A(t)$ and $B(t)$ as $C_{AB}(t, t') = \langle A(t)B(t') \rangle_0 - \langle A(t) \rangle_0 \langle B(t') \rangle_0$, where $\langle \dots \rangle_0$ denotes an equilibrium ensemble average. The conjugate linear response function $R_{AB}(t)$ is defined as

$$\langle A(t) \rangle - \langle A(t) \rangle_0 = f_0 \int_0^t R_{AB}(t, t') dt' + \mathcal{O}(f_0^2), \quad (1)$$

where $\langle \dots \rangle$ represents an average in the presence of the perturbation. The time integral, $\chi_{AB}(t, t') = \int_{t'}^t R_{AB}(t, u) du$, is the linear susceptibility, which is a more easily accessible quantity than R_{AB} both in experiments and simulations. In terms of χ_{AB} , the FDT becomes a simple linear relation

$$\chi_{AB}(t, t') = \frac{1}{T} [C_{AB}(t, t) - C_{AB}(t, t')] . \quad (2)$$

Far from equilibrium, the FDT has no reason to be obeyed. However, it has been shown that in systems with slow dynamics, like spin glasses or supercooled liquids, the linear relation eq. (2) is verified by replacing T by an *effective temperature* T_{eff} [26,27]. Technically, one introduces the fluctuation-dissipation ratio $X_{AB}(t, t')$ through [24]

$$R_{AB}(t, t') = \frac{X_{AB}(t, t')}{T} \frac{\partial}{\partial t'} C_{AB}(t, t'). \quad (3)$$

If $X_{AB}(t, t')$ is slaved to the relaxation and becomes a function of the variable $C_{AB}(t, t')$, an effective temperature $T_{\text{eff}}^{AB}(C) = T/X_{AB}(C)$ can then be defined from the slope of a “fluctuation-dissipation (FD) plot” of χ_{AB} vs. C_{AB} parametrized by the time difference $t - t'$. Such plots have repeatedly appeared in the literature of glassy materials. The equilibrium FDT is recovered when $X_{AB}(C) = 1$ and the slope of the parametric FD plot is then simply $-1/T$. The effective temperature defined above may in general depend on the chosen dynamic observables A and B but in order to allow for a thermodynamic interpretation, T_{eff} should be independent of this choice. This is of course the case in equilibrium and this hypothesis has been tested extensively in the glass literature [26,37,38].

We will investigate whether this important property also holds in our model. To this end, we first analyse the effect

of an external constant force $\mathbf{f}_i = \epsilon_i f_0 \mathbf{e}_x$ applied from time $t = 0$ in the x -direction, where $\epsilon_i = \pm 1$ with equal probability. In our simulations, the perturbation is introduced via the acceptance probability of a MC update,

$$P_{\text{acc}}(\delta \mathbf{x}_i, f_0) = \min[1, e^{\epsilon_i f_0 \delta x_i}] P_{\text{hard}}, \quad (4)$$

where $\delta x_i = \delta \mathbf{x}_i \cdot \mathbf{e}_x$ and the equilibrium temperature is $T = 1$. For $f_0 \neq 0$, this introduces a bias in the x -direction, whereas the motion in the transverse y -direction is unaffected. We carefully checked in all our simulations that the value of f_0 we use is small enough to probe the linear regime so that deviations from the equilibrium FDT relations are uniquely due to the non-equilibrium nature of the self-propelled dynamics. The associated susceptibility is the displacement of the particles induced by f_0 :

$$\chi_0(t) = \lim_{f_0 \rightarrow 0} \frac{1}{N} \sum_{i=1}^N \frac{\epsilon_i}{f_0} \langle x_i(t) - x_i(0) \rangle. \quad (5)$$

For these observables, the FDT in eq. (2) reads:

$$\chi_0(t) = \frac{1}{2T} \Delta x^2(t), \quad (6)$$

where $\Delta x^2(t) = N^{-1} \sum_{i=1}^N \langle (x_i(t) - x_i(0))^2 \rangle_0$ is the mean-squared displacement. In the long-time regime $\Delta x^2(t) \sim 2Dt$ and $\chi_0(t) \sim \mu t$, where D is the diffusion coefficient and μ the mobility. At long times, the FDT yields the Stokes-Einstein relation, which is generalized out-of-equilibrium to

$$T_{\text{eff}} = D/\mu, \quad (7)$$

with an effective temperature T_{eff} that in principle depends on both τ and φ .

In order to analyse carefully to what extent T_{eff} depends on the choice of observables, we consider also A_q and B_q defined as [37]

$$A_q(t) = \frac{1}{N} \sum_{j=1}^N \epsilon_j e^{iqx_j(t)}, \quad B_q(t) = 2 \sum_{j=1}^N \epsilon_j \cos[qx_j(t)], \quad (8)$$

where $x_j(t) = \mathbf{r}_j(t) \cdot \mathbf{e}_x$. With this choice, the associated correlation function entering in eq. (2) is the self-intermediate scattering function

$$F_s(q, t) = \frac{1}{N} \left\langle \sum_{j=1}^N e^{iq[x_j(t) - x_j(0)]} \right\rangle_0, \quad (9)$$

and the corresponding linear susceptibility is

$$\chi_q(t) = \lim_{f_0 \rightarrow 0} \langle A_q(t) - A_q(0) \rangle / f_0. \quad (10)$$

This perturbation is physically meaningful, as its wavevector dependence allows to probe the FDT at various length-scales. Numerically, we use

$$P_{\text{acc}}(\delta x_i, f_0) = \min[1, e^{2\epsilon_i f_0 [\cos(qx'_i) - \cos(qx_i)]}] P_{\text{hard}}, \quad (11)$$

where $x'_i = x_i + \delta x_i$. A non-equilibrium effective temperature $T_{\text{eff}} \neq 1$ is then revealed if a straight line appears in the FD plot χ_q vs. $[1 - F_s(q, t)]$ for a given value of q . In the limit of small q , the long-time diffusion is probed and these observables reduce to the Stokes-Einstein relation.

Effective temperatures in the active fluid. – In the dilute limit $\varphi \rightarrow 0$, the only control parameter is the persistence time τ . In this regime, particles have ballistic motion at short times, $t < \tau$, which crosses over to diffusive behaviour at long times, $t > \tau$, with $D \propto \tau$ [32]. The displacement χ_0 induced by a constant force does not depend on the noise correlations, and hence is also independent of the persistence time. The mobility is then equal to the one of non-persistent Brownian particles. Thus, from the Stokes-Einstein relation we find

$$T_{\text{eff}}(\tau, \varphi \rightarrow 0) = D/\mu \propto \tau. \quad (12)$$

This linear dependence on the persistence time obviously crosses over to a constant $T_{\text{eff}} \rightarrow 1$ as $\tau \rightarrow 0$ where equilibrium is recovered. Similar results were obtained before in a variety of active models [16, 17, 29].

Using the sedimentation of self-propelled particles, a meaningful T_{eff} should also be accessible from the density profiles $\varphi(z)$ along the direction of the gravity field. This has recently been investigated [8] experimentally in suspensions of Janus colloids and numerically using the present model. In the dilute limit, at the top of the sediment, both the Janus suspension and the self-propelled hard disk model were found to display an exponential density profile, just as an equilibrium ideal gas at temperature T_{eff} . Up to numerical accuracy, the effective temperature extracted from this static measurement is equal to the one obtained from the Stokes-Einstein relation. Thus, dilute suspensions of self-propelled particles can be seen as a “hot” ideal gas with effective temperature $T_{\text{eff}} \propto \tau$. The agreement between sedimentation and Stokes-Einstein relation is reasonable, as the gravity represents a biasing field acting at $q = 0$. Overall, this suggests that a *single-particle* effective temperature is useful to characterize dilute active particles at large enough length-scales, where details of the self-propulsion mechanism do not matter.

We now turn to finite densities, where many-body effects may modify the simple behaviour found in eq. (12). In Fig. 1(a-c), we show the results of numerical simulations for D , μ and T_{eff} for a broad range of τ and φ values. When $\varphi \rightarrow 0$, the leading behaviour exposed above is confirmed by the numerics. As discussed in detail in [32], the diffusion coefficient D at finite density is a non-monotonic function of the persistence time, and a density-dependent optimum value for a persistence time $\tau^*(\varphi)$ appears where the diffusivity is maximal, see Fig. 1(a). This maximum arises because self-propulsion simultaneously accelerates the dynamics of single particles, but it also leads to the formation of dynamic clusters where particles can be trapped. Physically, τ^* delimits the boundary between a homogeneous fluid phase and a cluster phase characterised by the

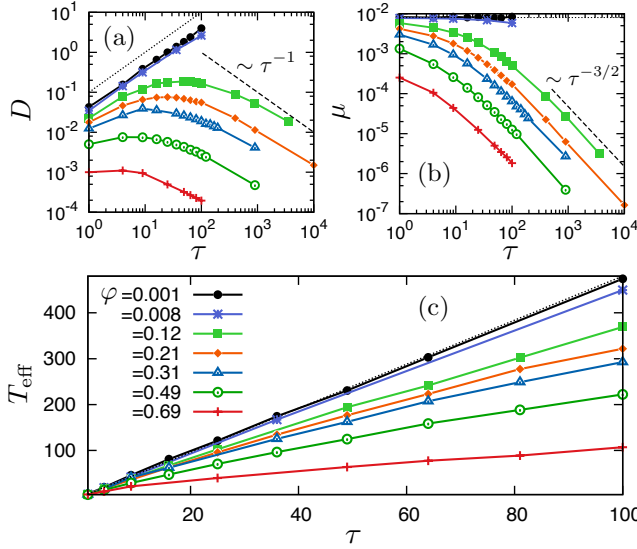


Fig. 1: Diffusivity (a), mobility (b) and effective temperature (c) as a function of τ for several packing fractions in the active fluid. In the dilute regime, $D \sim \tau$, $\mu \sim \text{const}$, $T_{\text{eff}} \sim \sqrt{\tau}$ (dotted lines). In the clustering regime, $D \sim \tau^{-1}$, $\mu \sim \tau^{-3/2}$, $T_{\text{eff}} \sim \sqrt{\tau}$ (dashed lines in (a) and (b)). The effective temperature increases with τ , but it decreases with φ .

presence of fractal aggregates. Deep in the cluster phase, the diffusivity decreases as $D \sim \tau^{-1}$, because it is controlled by the residence time of particles at the *surface* of the clusters [32].

By contrast, our simulations indicate that the mobility decreases monotonically with increasing τ at constant density, see Fig. 1(b). This simple behaviour arises because self-propulsion does not enhance the mobility of isolated particles but it strongly affects its value in the activity-induced cluster phase. Asymptotically, we find that $\mu \sim \tau^{-3/2}$, suggesting that μ is dominated by the average time spent by the particles *inside* the clusters. This behaviour can be understood by considering that particles either diffuse freely between the clusters with a diffusion constant given by $D(\varphi \rightarrow 0) \propto \tau$, or are kinetically trapped within clusters of average size $n \propto \sqrt{\tau}$ [32]. The time spent inside the clusters thus scales as $\tau \times n$, so that the mobility scales as $\tau^{-3/2}$, as observed numerically in the large- τ limit.

By taking the ratio of D and μ , we obtain the $q \rightarrow 0$ effective temperature shown in Fig. 1(c). The dilute limit behaviour $T_{\text{eff}} \sim \tau$ is numerically recovered. At finite density, we observe that T_{eff} increases monotonically with τ , and is thus not affected by the non-monotonic variation of the diffusion constant. However, the effect of the interactions at finite density is obvious as the effective temperature grows much more slowly with τ when $\varphi > 0$. In fact, the data shows that, for a fixed value of the persistence time, T_{eff} decreases strongly with φ , showing that interactions actually decrease the “agitation” of self-propelled particles. Indeed, in the strongly interacting regime, the

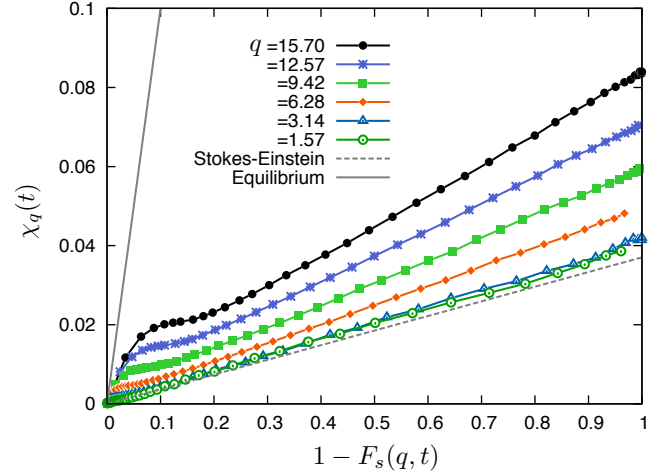


Fig. 2: Parametric FD plots obtained in the active fluid for $\tau = 9$ and $\varphi = 0.747$ for different values of the wavevector q characterizing the perturbation. Whereas the Stokes-Einstein value for T_{eff} is recovered in the $q \rightarrow 0$ limit, a different value of T_{eff} characterizes each q , suggesting that the active fluid regime is not characterized by a single effective temperature. Equilibrium FDT is shown as a full line.

combination of $D \sim \tau^{-1}$ and $\mu \sim \tau^{-3/2}$ suggests that $T_{\text{eff}}(\tau, \varphi) \sim \sqrt{\tau}$. Therefore, the scaling with persistence time *at finite density* is qualitatively different from the linear behaviour found in the dilute regime.

In a model of repulsive active dumbbells studied recently in the fluid regime, T_{eff} has a non-monotonic dependence on the activity that becomes more pronounced by increasing the density [18]. In our model, many-body effects alter the scaling of T_{eff} with τ in a simpler manner, monotonically reducing the effective “heating” of the system.

We now analyse perturbations at finite lengthscales, to probe more deeply the thermodynamic meaning of the effective temperature determined at large lengthscales from the Stokes-Einstein relation. In Fig. 2 we show representative parametric FD plots $\chi_q(t)$ versus $F_s(q, t)$ for our model at $\varphi = 0.747$ with a fixed $\tau = 9$ and several values of the wavevector q . As expected, the correlation and response functions of the system deviate strongly from the equilibrium FDT. However, the FD plots all follow a convincing straight line. This seems to imply that for each wavevector, a well-defined value of the effective temperature characterizes the long-time dynamics of the system. However, we also observe that the value of this effective temperature continuously depends on the chosen wavevector, and T_{eff} decreases when q is increased. This behaviour suggests that a unique effective temperature does not describe the dynamics of our model in the active fluid regime.

These observations extend to finite densities the results obtained analytically in the dilute regime of active Brownian particles, where it is similarly found that perturbations at finite lengthscales cannot be described in an ef-

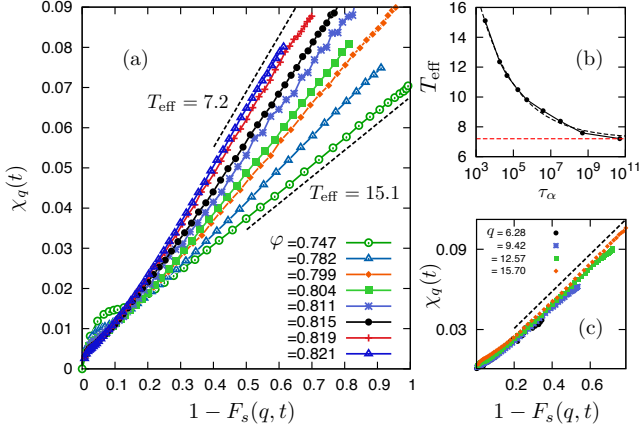


Fig. 3: (a): Parametric FD plots for $q = 4\pi$ and $\tau = 9$ and different volume fractions φ approaching the non-equilibrium glass transition. (b) Effective temperatures extracted from (a) plotted as a function of the relaxation time τ_α . The horizontal dotted line corresponds to the estimated asymptotic value of $T_{\text{eff}} = 7.2$ as $\tau_\alpha \rightarrow \infty$. The dashed line corresponds to an empirical power law fit, $T_{\text{eff}} = 7.2 + 42\tau_\alpha^{-0.2}$. (c) FD plots for $\tau = 9$, $\varphi = 0.819$ and different values of q . All wavevectors yield a unique value of the effective temperature $T_{\text{eff}} \approx 7.2$ (dashed line).

fective thermodynamical framework [17]. This conclusion therefore applies to the entire fluid regime, where T_{eff} sensitively depends on the choice of conjugate observables. More broadly, these results echo recent studies showing that extensions of equilibrium concepts to active fluids is in many instances not straightforward [20, 22, 23, 29, 39, 40].

Collective effective temperature in the glassy regime. — We finally investigate the model at very high densities, approaching dynamical arrest from the fluid. Recent work supports the idea that dense assemblies of self-propelled particles can display a dramatic slow down of the dynamics sharing strong analogies with the glassy dynamics of particle systems in contact with a thermal bath [33, 35, 41–45]. It was found in particular that activity shifts the glass transition towards higher densities (or lower temperatures), but leaves the main collective properties of the slow relaxation near the transition qualitatively unchanged [33, 41, 42].

We compute the susceptibility $\chi_q(t)$ and correlations $F_s(q, t)$ associated to a modulated perturbation of wavevector q in dense suspensions of self-propelled disks. We focus first on the parametric FD plots for fixed $q = 4\pi$, $\tau = 9$ and several packing fractions from $\varphi = 0.747$ (liquid regime) to $\varphi = 0.821$ (very close to the non-equilibrium glass transition $\varphi_c(\tau = 9) \approx 0.823$). The results are displayed in Fig. 3. Similar results are found for other values of the persistence time.

After a relatively short time corresponding to $F_s(q, t \approx \tau) \approx 0.85$ the FD plots for different packing fractions are well-described by straight lines with a slope that evolves

slowly with φ . In the density regime investigated, T_{eff} decreases from $T_{\text{eff}} \approx 15$ to $T_{\text{eff}} \approx 7$ over a density regime where the relaxation time increases by roughly seven orders of magnitude. The short-time period corresponding to the non-thermal part of the FD plot is a distinctive feature of active systems. In aging glassy systems, this crossover corresponds to the two-step decay of correlation functions with an intermediate plateau regime. Our system presents a two-step decay of $F_s(q, t)$ as well [31], but the plateau value of the correlation function plays no role in the FD plots. Instead, deviations from equilibrium are controlled by the timescale of the self-propulsion mechanism, an effective temperature appearing when $t \gg \tau$. As similar trend was noted in mean-field calculations [41].

From the data in Fig. 3(a) we extract the value of the effective temperature and present its evolution with density in Fig. 3(b). To better appreciate the distance to the glass transition we simultaneously measure the structural relaxation time τ_α of the system defined as $F_s(q_{\text{max}}, \tau_\alpha) = 0.2$, and represent T_{eff} as a function of τ_α ; q_{max} corresponds to the first peak of the static structure factor. These results show that T_{eff} decays as dynamical arrest is approached, and we estimate that it approaches an asymptotic value $T_{\text{eff}} \approx 7.2$ as $\tau_\alpha \rightarrow \infty$, which clearly differs from the equilibrium value. Therefore we see that the persistence time τ not only shifts the location of the glass transition towards large densities, it also fixes the value of the effective temperature at the glass transition.

The crucial prediction of the mean-field theory of glassy dynamics is the observable-independence of the effective temperature. To test this, we compute $\chi_q(t)$ and $F_s(q, t)$ for several different wavevectors at fixed $\tau = 9$ and $\varphi = 0.819$. Remarkably, the results shown in Fig. 3 are consistent with a *unique* effective temperature, as the FD plots for different q are almost superimposed. In particular, the difference with the data at lower density in Fig. 2 is striking. Numerically, the trend is that the q -dependence observed in the fluid becomes less and less pronounced as the density is increased towards the glassy phase, in perfect agreement with mean-field predictions.

Conclusion. — The central result of the present work is the numerical confirmation in a finite dimensional model of self-propelled particles that a collective effective temperature emerges in active systems near a non-equilibrium glass transition. We have also shown that this physical picture does not apply in the active fluid at small and moderate densities, where only perturbations at large enough lengthscales appear effectively “thermal”, whereas finite lengthscales perturbations are not well described by an effective thermodynamical treatment.

Physically, the key aspect of active glassy systems that allows a meaningful definition of the effective temperature, is a clear separation of timescales between microscopic dynamics at small timescales that is highly sensitive to details of the self-propulsion and the structural relaxation taking place at much larger timescales. It is the long-time

sector for which the definition of an effective temperature appears meaningful. In addition, because the system undergoes a simultaneous kinetic freezing of all degrees of freedom near the glass transition, the effective temperature becomes independent of the probed lengthscales and is thus essentially shared by all of them.

* * *

The research leading to these results has received funding from the European Research Council under the European Union's Seventh Framework Programme (FP7/2007-2013) / ERC Grant agreement No 306845.

REFERENCES

- [1] D. Chandler. *Introduction to Modern Statistical Mechanics*. Oxford University Press, 1987.
- [2] J. Kurchan. *Nature*, 433:222, 2005.
- [3] T. E. Angelini, E. Hannezo, X. Trepot, M. Marquez, J. J. Fredberg, and D. A. Weitz. *PNAS*, 108(12):4714–9, 2011.
- [4] X-L. Wu and A. Libchaber. *Phys. Rev. Lett.*, 84:3017, 2000.
- [5] J. Palacci, C. Cottin-Bizonne, C. Ybert, and L. Bocquet. *Phys. Rev. Lett.*, 105(8):088304, 2010.
- [6] I. Theurkauff, C. Cottin-Bizonne, J. Palacci, C. Ybert, and L. Bocquet. *Phys. Rev. Lett.*, 108(26):268303, 2012.
- [7] I. Buttinoni, J. Bialké, F. Kümmel, H. Löwen, C. Bechinger, and T. Speck. *Phys. Rev. Lett.*, 110(23):238301, 2013.
- [8] F. Ginot, I. Theurkauff, D. Levis, C. Ybert, L. Bocquet, L. Berthier, and C. Cottin-Bizonne. *Phys. Rev. X*, 5:011004, 2015.
- [9] J. Deseigne, O. Dauchot, and H. Chaté. *Phys. Rev. Lett.*, 105:098001, 2010.
- [10] V. Narayan, S. Ramaswamy, and N. Menon. *Science*, 317:105, 2007.
- [11] M. C. Marchetti, J. F. Joanny, S. Ramaswamy, T. B. Liverpool, J. Prost, M. Rao, and R. Aditi Simha. *Rev. Mod. Phys.*, 85:1143, 2013.
- [12] T. Vicsek and A. Zafeiris. *Physics Reports*, 517:71–140, 2012.
- [13] D. Loi, S. Mossa, and L. F. Cugliandolo. *Phys. Rev. E*, 77:051111, 2008.
- [14] S. Wang and P. G. Wolynes. *J. Chem. Phys.*, 135(5):051101, 2011.
- [15] D. Loi, S. Mossa, and L. F. Cugliandolo. *Soft Matter*, 7:10193, 2011.
- [16] E. Ben-Isaac, Y-K. Park, G. Popescu, F. Brown, N. Gov, and Y. Shokef. *Phys. Rev. Lett.*, 106:238103, 2011.
- [17] G. Szamel. *Phys. Rev. E*, 90(1):012111, 2014.
- [18] A. Suma, G. Gonnella, G. Laghezza, A. Lamura, A. Mossa, and L. F. Cugliandolo. *Phys. Rev. E*, 90(5):052130, 2014.
- [19] S. C. Takatori, W. Yan, and J. F. Brady. *Phys. Rev. Lett.*, 113(2):028103, 2014.
- [20] A. P. Solon, Y. Fily, A. Baskaran, M. E. Cates, Y. Kafri, M. Kardar, and J. Tailleur. *arXiv: 1412.3952*, 2014.
- [21] T. F. F. Farage, P. Krinninger, and J. M. Brader. *Phys. Rev. E*, 91:042310, 2015.
- [22] J. Tailleur and M. E. Cates. *Phys. Rev. Lett.*, 100:218103, 2008.
- [23] J. Bialké, H. Löwen, and T. Speck. *arXiv:1412.4601*, 2014.
- [24] L. F. Cugliandolo and J. Kurchan. *Phys. Rev. Lett.*, 71:173, 1993.
- [25] L. F. Cugliandolo and J. Kurchan. *J. Phys. A: Math. Theor.*, 27:5749, 1994.
- [26] A. Crisanti and F. Ritort. *J. Phys. A: Math. Theor.*, 36:R181, 2003.
- [27] L. F. Cugliandolo. *J. Phys. A: Math. Theor.*, 44(48):483001, 2011.
- [28] L. F. Cugliandolo, J. Kurchan, and L. Peliti. *Phys. Rev. E*, 55:3898, 1997.
- [29] J. Tailleur and M. E. Cates. *EPL*, 86:60002, 2009.
- [30] C. Maggi, M. Paoluzzi, N. Pellicciotta, A. Lepore, L. Angelani, and R. Di Leonardo. *Phys. Rev. Lett.*, 23(113):238303, 2014.
- [31] L. Berthier and J. Kurchan. *Nature Physics*, 9(5):310–314, 2013.
- [32] D. Levis and L. Berthier. *Phys. Rev. E*, 89(6):062301, 2014.
- [33] L. Berthier. *Phys. Rev. Lett.*, 112(22):220602, 2014.
- [34] W. Krauth. *Statistical Mechanics: Algorithms and Computations*. Oxford University Press, 2006.
- [35] G. Szamel, E. Flenner, and L. Berthier. *Phys. Rev. E*, 91:062304, 2015.
- [36] A. Donev, F. H. Stillinger, and S. Torquato. *Phys. Rev. Lett.*, 96:0603183, 2006.
- [37] L. Berthier and J-L. Barrat. *J. Chem. Phys.*, 116(14):6228, 2002.
- [38] S. Fielding and S. Sollich. *Phys. Rev. Lett.*, 88:050603, 2002.
- [39] G. S. Redner, M. F. Hagan, and A. Baskaran. *Phys. Rev. Lett.*, 110:055701, 2013.
- [40] Y. Fily and M. C. Marchetti. *Phys. Rev. Lett.*, 108(23):235702, 2012.
- [41] L. Berthier and J. Kurchan. *Nature Physics*, 9(1):310–314, 2013.
- [42] R. Ni, M. A. Cohen Stuart, and M. Dijkstra. *Nature Comm.*, 4:2704, 2013.
- [43] A. Wysocki, R. G. Winkler, and G. Gompper. *EPL*, 105:48004, 2014.
- [44] T. F. F. Farage and J. M. Brader. *arXiv:1403.0928*, 2014.
- [45] R. Mandal, P. J. Bhuyan, M. Rao, and C. Dasgupta. *arXiv:1412.1631*, 2014.